Transmit Antenna Subset Selection in Spatial Modulation Relying on a Realistic Error-Infested Feedback Channel

Rakshith Rajashekar, *Member, IEEE*, K.V.S. Hari, *Fellow, IEEE* and L. Hanzo, *Fellow, IEEE*

***Abstract*—In this paper, we study the performance of spatial modulation (SM) employing Euclidean distance based antenna selection (EDAS) operating in a realistic error-infested feedback channel, which has hitherto only been studied under ideal feedback channel conditions. Specifically, we model the feedback channel by a bit-flip probability δ and study its impact on the forward link employing EDAS. We show that the erroneous feedback channel severely degrades the performance of EDAS-aided SM (EDAS-SM) system by imposing an error floor in the forward link. Furthermore, we quantify the error floors associated both with the spatial and with the conventional symbols with the aid of asymptotic symbol error rate analysis. The expressions derived for the error floors in the forward link are utilised for optimizing the feedback signalling, which are shown to help reduce the error floor levels. Furthermore, a pilot-aided selection verification (PSV) algorithm is proposed for mitigating the effects of antenna-set mismatch between the transmitter and the receiver, which eliminates the error floor in the forward link. Simulations are conducted in order to validate the theoretical results presented in the paper. Furthermore, the bit-error ratio (BER) performance of the EDAS-SM is compared to that of the conventional antenna selection (C-AS) both in the PSV as well as in the no selection verification scenarios. It is observed that EDAS-SM outperforms C-AS in both the scenarios considered. Specifically, at a BER of 10^{-5}, EDAS-SM is observed to give a 3dB signal-to-noise ratio gain compared to the C-AS, when operating at a spectral efficiency of 7 bits per channel use in the face of a feedback BER of $\delta = 0.05$.**

***Index Terms*—Antenna subset selection, diversity gain, erroneous feedback, Euclidean distance, error floor.**

List of Acronyms

BER	Bit Error Ratio
C-AS	Conventional Antenna Selection
ED	Euclidean Distance
EDAS	Euclidean Distance based Antenna Selection
EDAS-SM	Euclidean Distance based Antenna Selection aided Spatial Modulation
EFC	Erroneous Feedback Channel
ICI	Inter Channel Interference
MAP	Mirror Activation Pattern
MIMO	Multiple Input Multiple Output
OSA	Optimized Signaling Assignment
PSV	Pilot-aided Selection Verification
RF	Radio Frequency
SER	Symbol Error Rate
SNR	Signal-to-Noise Ratio
SM	Spatial Modulation
TA	Transmit Antenna

List of Symbols

δ	Bit-flip probability of the feedback channel
$d_H(\mathbf{w}, \mathbf{w}')$	Hamming distance between the codewords $\mathbf{w}$ and $\mathbf{w}'$
$g(\cdot)$	Bijective map from $\mathcal{I}$ to $\mathcal{W}$
$\mathcal{I}$	Set of enumerations of all possible $\binom{N_t}{N_{SM}}$ antenna combinations
I_k	k^{th} antenna combination in the set $\mathcal{I}$
M	Size of the PSK/QAM signal set
n	Number of possible antenna combinations
N_t	Number of TAs
N_r	Number of receive antennas
N_{SM}	Number of TAs used for SM
$\mathsf{P_e}(SM)$	SM symbol error probability
$\mathsf{P_e}(\mathcal{A})$	Antenna index error probability
$\mathsf{P_e}(S, \mathcal{A}^c)$	Symbol error rate when there is no antenna index error
$\mathsf{P_e^{EFC}}(SM)$	SM symbol error probability when operating in EFC
$\mathsf{P_e^{EFC}}(\mathcal{A})$	Antenna index error probability when operating in EFC
$\mathsf{P_e^{EFC}}(S, \mathcal{A}^c)$	Symbol error rate when there is no antenna index error while operating in EFC
ρ	SNR at each receive antenna
$\mathcal{W}$	Set of m-bit binary codewords
$\mathcal{X}$	Set of all possible transmit vectors

I. Introduction

Multi-antenna transmission schemes support reliable, high data rate wireless communication, albeit at the cost of significant hardware complexity, mainly due to the multiple radio frequency (RF) chains required at both the transmitter as well as the receiver. Antenna selection is a low-complexity solution that alleviates the requirement of multiple RF chains, while still exploiting the benefits of multiple antennas [1]-[6]. Spatial

R. Rajashekar and L. Hanzo are with the School of ECS, University of Southampton, UK (e-mail: rmr1u14@soton.ac.uk, lh@ecs.soton.ac.uk).

K.V.S. Hari is with the Dept. of ECE, Indian Institute of Science, Bangalore, India (e-mail: hari@ece.iisc.ernet.in).

The financial support of the EPSRC projects EP/Noo4558/1 and EP/L018659/1, as well as of the European Research Council's Advanced Fellow Grant under the Beam-Me-Up project and of the Royal Society's Wolfson Research Merit Award is gratefully acknowledged.

modulation (SM) [7]-[17] is a relatively new multiple-input multiple-output (MIMO) transmission scheme conceived for reducing the hardware complexity at the transmitter, which employs a single RF chain, whilst conventional MIMO systems [18] require multiple RF chains. Specifically, the SM system activates only a single transmit antenna (TA) out of N_{SM} antennas in each channel use, where the choice of the active TA is based on the data bits to be transmitted. Furthermore, a symbol selected from a conventional signal set such as QAM/PSK is transmitted over the TA activated. Specifically, the information bit stream is divided into blocks of length $\log_2(N_{SM}M)$ bits, and in each block, $\log_2(M)$ bits select a symbol s from an M-ary signal set (such as M-QAM or -PSK). Furthermore, $\log_2(N_{SM})$ bits select an antenna out of N_{SM} transmit antennas for the transmission of the symbol s. The throughput achieved by this scheme is $R_{SM} = \log_2(N_{SM}M)$ bits per channel use (bpcu). Since only a single TA is activated in each channel use, the SM system completely eliminates the inter-channel interference (ICI) at the receiver, thereby facilitating low-complexity single-stream ML detection [14]. The benefits of energy efficient transmitter and of low-complexity optimal detection at the receiver have promoted the SM scheme to an attractive candidate for next-generation wireless systems [16], [17].

One of the limitations of the SM scheme is that it suffers from the lack of transmit diversity gain owing to having a single RF chain at the transmitter. Hence, several open- and closed-loop techniques were conceived in the literature for overcoming this impediment. The open-loop techniques mainly constitute employing space-time block coding [19] aided SM schemes, which include 1) an Alamouti code [20] aided SM scheme conceived in [21], 2) a complex interleaved orthogonal design proposed in [22], 3) an SM scheme employing Alamouti STBC in a cyclic structure proposed in [23], 4) an SM scheme relying on Alamouti STBC with temporal permutations conceived in [24], etc. All the aforementioned schemes achieve a transmit diversity order of two, while requiring two transmit RF chains, except for the scheme in [22], which requires a single transmit RF chain.

The existing closed-loop techniques mainly rely on modulation-order and antenna-subset selection schemes [25]-[34]. Specifically, a link-adaptive modulation scheme was proposed by Yang *et. al.* in [25], while both capacity based and Euclidean distance (ED) based antenna selection (EDAS) schemes were conceived by Rajashekar *et. al.* in [26]. Their performances were studied under imperfect channel conditions in [27]. Furthermore, low-complexity antenna selection algorithms were proposed by Zhau and Wang in [28], [29], respectively. The transmit diversity order of EDAS was quantified by Rajashekar *et. al.* in [30], while Sun *et. al.* proposed a cross-entropy based method for reducing the search complexity of EDAS in [31]. In [32], Yang *et. al.* proposed an improved low-complexity implementation of EDAS by striking a beneficial performance vs. complexity trade-off. Recently, Sun *et. al.* [33] have proposed a reduced-dimensional EDAS-equivalent criterion, which results in the same performance as that of EDAS, albeit at a reduced complexity. In [34], Naresh *et. al.* have studied the ED based mirror activation pattern selection schemes in the context of RF-mirror aided spatial modulation systems. While all the above schemes were studied in the frequency-flat fading scenario, recently Rajashekar *et. al.* have proposed EDAS for realistic frequency selective scenarios [35] with the aid of a partial interference cancellation receiver [12]. Table I summarizes the various closed-loop SM transmission schemes discussed so far.

Against this background, the following are the contributions of this paper:

1) All the closed-loop SM schemes discussed above assume that the feedback channel is error-free, whereas in practical scenarios the feedback channel is often error-infested. For example, in third-generation (3G) systems [36] the feedback information is uncoded and bit-error rates as high as 4% are common. A detailed study of the detrimental effects of erroneous feedback channels (EFC) in case of conventional antenna selection (C-AS) can be found in [6]. In this paper, we study the performance of EDAS in SM systems by considering an EFC that models the practical operating conditions, which has hitherto not been studied in the literature.
2) Erroneous feedback causes mismatch between the antenna subset requested by the receiver and that used by the transmitter. This in turn imposes severe degradation on the performance of EDAS in the forward link, resulting in error floors. We provide a theoretical analysis of the asymptotic symbol error rate (SER) and quantify the error floor when operating with an EFC. Furthermore, with the aid of the analytical results derived, we optimize the feedback signalling assignment so as to reduce the detrimental effects of feedback errors on the forward link.
3) Lastly, we propose a low-complexity pilot aided selection verification scheme for the receiver, which ensures that the receiver uses the same set of antennas as that used by the transmitter and hence overcomes the error floor in the forward link. Furthermore, we show with the aid of simulation results that the EDAS aided SM scheme is quite robust to feedback errors, when compared to C-AS, and hence attains a better bit error ratio (BER) performance.

The remainder of the paper is organized as follows. The system model and the EFC model are presented in Section II. The asymptotic SER analysis of the EDAS aided SM system operating in an EFC as well as the proposed selection verification algorithm is presented. Our simulation results are discussed in Section IV, while Section V concludes the paper.

Notations: $\mathbb{C}$ and $\mathbb{R}$ represent the field of complex and real numbers, respectively. The uppercase boldface letters represent matrices and lowercase boldface letters represent vectors. The notations of $\|\cdot\|_F$ and $\|\cdot\|$ represent the Frobenious norm of a matrix and the two-norm of a vector, respectively. The notations of $(\cdot)^H$ and $(\cdot)^T$ indicate the Hermitian transpose and transpose of a vector/matrix, respectively, while $|\cdot|$ represents the magnitude of a complex quantity, or the cardinality of a given set. A circularly symmetric complex-valued Gaussian distribution with a mean of μ and a variance of σ^2 is

TABLE I
SUMMARY OF THE VARIOUS EXISTING CLOSED-LOOP SM TRANSMISSION SCHEMES.

	Contributions
P. Yang *et. al.* [25]	Link adaptive SM based on modulation order selection were proposed, where both signal and spatial constellation sizes are chosen based on the channel condition.
R. Rajashekar *et. al.* [26], [27]	Capacity optimized and Euclidean distance based TAS schemes for SM systems were proposed and studied in perfect and imperfect CSIR conditions.
Z. Zhau *et. al.* [28]	Reduced complexity TAS schemes based on pairwise symbol error probability and antenna correlation information were proposed.
N. Wang *et. al.* [29]	The computational complexity of EDAS was further reduced by exploiting the rotational symmetry in the signal constellation.
R. Rajashekar *et. al.* [30]	The achievable transmit diversity order by the EDAS was quantified.
Z. Sun *et. al.* [31]	The EDAS problem was reformulated as a combinatorial optimization problem, which was solved by employing the cross-entropy method that imposes low-complexity compared to the optimal EDAS.
P. Yang *et. al.* [32]	A QR decomposition and error vector magnitude based TAS schemes were proposed as alternate low-complexity solutions to EDAS.
Z. Sun *et. al.* [33]	Relying on matrix dimension reduction, an EDAS-equivalent criterion was developed and the computational complexity of EDAS was reduced by tree search and decremental TAS schemes.
Y. Naresh *et. al.* [34]	Media based modulation with mirror activation pattern (MAP) selection based on a Euclidean distance (ED)-based metric was studied.
R. Rajashekar *et. al.* [35]	EDAS for frequency-selective fading scenario was proposed with the aid of partial interference cancellation receiver [12].

Note : All the above schemes assume an idealistic error-free feedback channel.

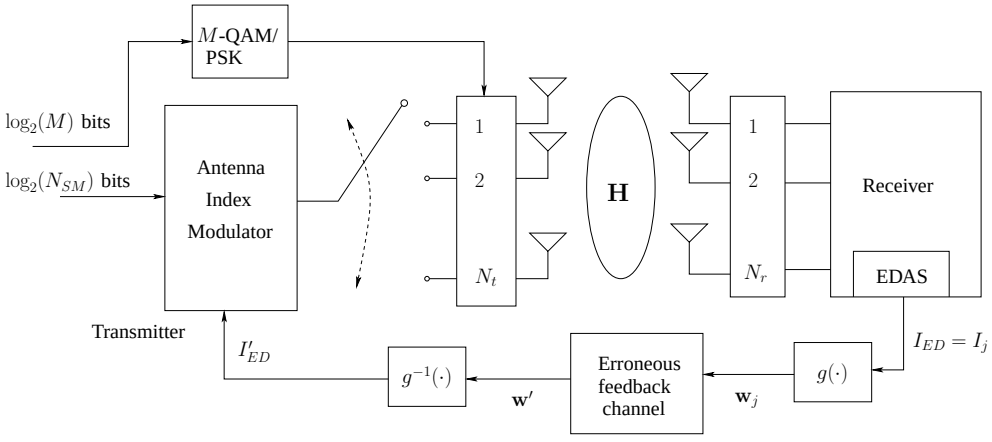

Fig. 1. Pictorial depiction of the EDAS aided SM system operating in an erroneous feedback channel.

represented by $\mathcal{CN}(\mu, \sigma^2)$.

II. System Model

In this section, we briefly describe the SM system model operating with the aid of EDAS as well as the EFC used in the paper.

A. SM System with EDAS

Consider an SM system having N_t transmit as well as N_r receive antennas and equipped with a single RF chain at the transmitter. Let $N_{SM} < N_t$ antennas be used for SM, where N_{SM} is assumed to be a power of two. The received vector when a symbol s transmitted from the i^{th} transmit antenna is given by

$$\mathbf{y} = \sqrt{\rho}\mathbf{h}_i s + \mathbf{n}, \tag{1}$$

where $\mathbf{y} \in \mathbb{C}^{N_r}$ is the received signal vector, ρ is the average signal-to-noise ratio (SNR) at each receive antenna, s is a complex-valued symbol selected from a unit-energy M-QAM or -PSK signal set represented by S, $\mathbf{h}_i \in \mathbb{C}^{N_r}$ is the channel vector corresponding to the i^{th} transmit antenna, and $\mathbf{n} \in \mathbb{C}^{N_r}$ is the noise vector. The entries of both the channel matrix $\mathbf{H} = [\mathbf{h}_1, \mathbf{h}_2, \ldots, \mathbf{h}_{N_t}] \in \mathbb{C}^{N_r \times N_t}$ and of the noise $\mathbf{n}$ are from $\mathcal{CN}(0, 1)$. Each block of $\log_2(MN_{SM})$ bits in the input bit stream is divided into blocks of $\log_2(M)$ bits that select a symbol from an M-QAM or -PSK signal set and $\log_2 N_{SM}$ bits select an antenna i out of N_{SM} transmit antennas for the transmission of the selected symbol s.

EDAS [26]: Let $\mathcal{I} = \{I_1, I_2, \ldots, I_n\}$ represent the set of enumerations of all possible $n = \binom{N_t}{N_{SM}}$ combinations of selecting N_{SM} out of N_t antennas. The ED optimized antenna subset is obtained as follows:

$$I_{ED} = \arg\max_{I \in \mathcal{I}} \left\{ \min_{\mathbf{x}_1 \neq \mathbf{x}_2 \in \mathcal{X}} \|\mathbf{H}_I(\mathbf{x}_1 - \mathbf{x}_2)\|^2 \right\}, \tag{2}$$

where $\mathcal{X}$ represents the set of all possible transmit vectors given by $\{s\mathbf{e}_1, s\mathbf{e}_2, \ldots, s\mathbf{e}_{N_{SM}}\}$, where $\mathbf{e}_i$ is the i^{th} column of $\mathbf{I}_{N_{SM}}$. The matrix $\mathbf{H}_I \in \mathbb{C}^{N_r \times N_{SM}}$ corresponds to the channel matrix $\mathbf{H}$ with columns given by I. The ED-optimized antenna subset I_{ED} obtained from (2) is encoded into bits and fed back to the transmitter in the feedback channel. Upon receiving I_{ED}, the transmitter uses the antennas indexed by I_{ED} for SM in the subsequent data transmissions. Figure 1 gives a pictorial representation of the EDAS aided SM system operating in an erroneous feedback channel.

B. Feedback Channel Model

Let $\mathcal{W}$ represent a set of binary codewords $\{\mathbf{w}_1, \mathbf{w}_2, \ldots, \mathbf{w}_n\}$ each comprising $m = \lceil \log_2 n \rceil$ bits[1] and $g : \mathcal{I} \rightarrow \mathcal{W}$ represent a bijective map from the set of antenna subsets $\mathcal{I}$ to the set of binary codewords $\mathcal{W}$, i.e. $g(I_j) = g(I_k)$ iff $I_k = I_j$. Upon obtaining the ED optimized antenna subset $I_{ED} = I_j$, the receiver obtains the associated codeword $g(I_j) = \mathbf{w}_j$ and transmits it over the feedback link to the transmitter. Due to the EFC, the received codeword $\mathbf{w}'$ at the transmitter would be different from the one transmitted by the receiver, as depicted in Fig. 1. If δ is the bit-flip probability in the feedback channel, the probability of pairwise codeword error in the feedback link is given by

$$\mathsf{Pr}(\mathbf{w}_i, \mathbf{w}_j) = \delta^{d_H(\mathbf{w}_i, \mathbf{w}_j)}(1-\delta)^{m - d_H(\mathbf{w}_i, \mathbf{w}_j)}, \tag{3}$$

where $d_H(\mathbf{w}_i, \mathbf{w}_j)$ is the Hamming distance between the codewords $\mathbf{w}_i$ and $\mathbf{w}_j$. Furthermore, we assume that when the transmitter receives an illegitimate codeword due to a feedback channel error, it discards it and initiates a new antenna subset selection procedure at the receiver and waits for a legitimate codeword to be received over the feedback link. Thus, the codeword errors induced by the feedback channel result in only legitimate codewords being processed by the transmitter. Note that the feedback channel model assumed in this paper is similar to that assumed in [6].

III. Asymptotic SER Analysis of EDAS aided SM system operating with Erroneous Feedback Channel

In this section, we present the asymptotic SER analysis of the EDAS aided SM system and quantify the error floors in the forward link caused by the EFC. Before proceeding further, let us introduce the following distance measures that are used in our derivations.

Definition 1: Consider two equal-sized sets A and B, whose elements are indexed from $1, 2, \ldots, |A|$. Let $(A \cap B)_I$ represent a set containing only those elements of $A \cap B$, which do not share the same indices in each of the sets.

For example, given $A = \{1, 2, 3, 4, 5, 8\}$ and $B = \{3, 4, 5, 6, 7, 8\}$, we have $A \cap B = \{3, 4, 5, 8\}$ and $(A \cap B)_I = \{3, 4, 5\}$.

Definition 2: Given two antenna subsets I_i and I_j of size N_{SM}, let $d_I(I_i, I_j) = |(I_i \cap I_j)_I|$ and $d_U(I_i, I_j) = |I_i \backslash (I_i \cap I_j)| = |I_j \backslash (I_i \cap I_j)|$.

In the example considered above, we have $d_I(A, B) = 3$ and $d_U(A, B) = 2$.

A. SER Analysis of EDAS in Erroneous Feedback Channel

Let I_{ED} represent the EDAS-optimized antenna subset requested by the receiver and I'_{ED} represent the antenna subset used by the transmitter. For convenience, we use I and I' to denote the antenna subsets I_{ED} and I'_{ED}, respectively.

The probability of the SM symbol error in the forward link when operating with an EFC can be written as

$$\mathsf{P}_{\mathsf{e}}^{\mathsf{EFC}}(SM) = \sum_{I \in \mathcal{I}} \sum_{I' \in \mathcal{I}} \mathsf{P}_{\mathsf{e}}(SM | I', I) \mathsf{Pr}(I', I), \tag{4}$$

$$= \sum_{I \in \mathcal{I}} \sum_{I' \in \mathcal{I}} \mathsf{P}_{\mathsf{e}}(SM | I', I) \mathsf{Pr}(I' | I) \mathsf{Pr}(I). \tag{5}$$

Considering the fact that all the channel coefficients are identically distributed, we have $\mathsf{Pr}(I) = 1/n \ \forall \ I \in \mathcal{I}$, i.e. all the antenna subsets are equally likely. Furthermore, we have $\mathsf{Pr}(I' = I_i | I = I_j) = \mathsf{Pr}(g(I_i), g(I_j)) = \mathsf{Pr}(\mathbf{w}_i, \mathbf{w}_j)$ and $\mathsf{P}_{\mathsf{e}}(SM | I', I) = \mathsf{P}_{\mathsf{e}}(\mathcal{A} | I', I) + \mathsf{P}_{\mathsf{e}}(S, \mathcal{A}^c | I', I)$, where the first term corresponds to the antenna index error, while the second

[1]Since $n = \binom{N_t}{N_{SM}}$ is not a power of two, not all m-bit binary sequences are legitimate codewords.

term corresponds to the symbol error under the condition that there is no antenna index error. Thus, (5) can be written as

$$\mathsf{P}_{\mathsf{e}}^{\mathsf{EFC}}(SM) = \mathsf{P}_{\mathsf{e}}^{\mathsf{EFC}}(\mathcal{A}) + \mathsf{P}_{\mathsf{e}}^{\mathsf{EFC}}(S,\mathcal{A}^c), \tag{6}$$

$$= \frac{1}{n}\sum_{I\in\mathcal{I}}\sum_{I'\in\mathcal{I}} \mathsf{P}_{\mathsf{e}}(\mathcal{A}|I',I)\mathsf{Pr}[g(I),g(I')] + \frac{1}{n}\sum_{I\in\mathcal{I}}\sum_{I'\in\mathcal{I}} \mathsf{P}_{\mathsf{e}}(S,\mathcal{A}^c|I',I)\mathsf{Pr}[g(I),g(I')], \tag{7}$$

$$= \frac{1}{n}\sum_{I'=I\in\mathcal{I}} \mathsf{P}_{\mathsf{e}}(\mathcal{A}|I',I)\mathsf{Pr}(g(I),g(I')) + \frac{1}{n}\sum_{I'=I\in\mathcal{I}} \mathsf{P}_{\mathsf{e}}(S,\mathcal{A}^c|I',I)\mathsf{Pr}[g(I),g(I')] + \frac{1}{n}\sum_{I\in\mathcal{I}}\sum_{I\neq I'\in\mathcal{I}} \mathsf{P}_{\mathsf{e}}(\mathcal{A}|I',I)\mathsf{Pr}[g(I),g(I')] + \frac{1}{n}\sum_{I\in\mathcal{I}}\sum_{I\neq I'\in\mathcal{I}} \mathsf{P}_{\mathsf{e}}(S,\mathcal{A}^c|I',I)\mathsf{Pr}[g(I),g(I')], \tag{8}$$

$$= \frac{1}{n}\sum_{I\in\mathcal{I}} \mathsf{P}_{\mathsf{e}}(SM|I'=I,I)\mathsf{Pr}[g(I),g(I)] + \frac{1}{n}\sum_{I\in\mathcal{I}}\sum_{I\neq I'\in\mathcal{I}} \mathsf{P}_{\mathsf{e}}(\mathcal{A}|I',I)\mathsf{Pr}[g(I),g(I')] + \frac{1}{n}\sum_{I\in\mathcal{I}}\sum_{I\neq I'\in\mathcal{I}} \mathsf{P}_{\mathsf{e}}(S,\mathcal{A}^c|I',I)\mathsf{Pr}[g(I),g(I')]. \tag{9}$$

The first term in (9) corresponds to the case, where there is no feedback error, whereas the next two terms correspond to the case, where the antenna subset requested by the receiver differs from that used by the transmitter owing to the feedback channel error. We have

$$\lim_{\rho\to\infty}\frac{1}{n}\sum_{I\in\mathcal{I}} \mathsf{P}_{\mathsf{e}}(SM|I'=I,I)\mathsf{Pr}[g(I),g(I)] = 0, \tag{10}$$

since $\lim_{\rho\to\infty}\mathsf{P}_{\mathsf{e}}(SM|I'=I,I) = 0 \;\forall\; I\in\mathcal{I}$, where $\mathsf{P}_{\mathsf{e}}(SM|I'=I,I) = \mathsf{P}_{\mathsf{e}}(SM) < c/\rho^{N_r(N_t-N_{SM}+1)}$ (Prop. 1 and Prop. 2 in [30]). Hence, the first term in (9) vanishes when $\rho\to\infty$. Thus, we have

$$\lim_{\rho\to\infty}\mathsf{P}_{\mathsf{e}}^{\mathsf{EFC}}(SM) = \lim_{\rho\to\infty}\mathsf{P}_{\mathsf{e}}^{\mathsf{EFC}}(\mathcal{A}) + \lim_{\rho\to\infty}\mathsf{P}_{\mathsf{e}}^{\mathsf{EFC}}(S,\mathcal{A}^c),$$

where

$$\lim_{\rho\to\infty}\mathsf{P}_{\mathsf{e}}^{\mathsf{EFC}}(\mathcal{A}) \equiv \lim_{\rho\to\infty}\frac{1}{n}\sum_{I\in\mathcal{I}}\sum_{I\neq I'\in\mathcal{I}} \mathsf{P}_{\mathsf{e}}(\mathcal{A}|I',I) \times \mathsf{Pr}[g(I),g(I')], \tag{11}$$

and

$$\lim_{\rho\to\infty}\mathsf{P}_{\mathsf{e}}^{\mathsf{EFC}}(S,\mathcal{A}^c) \equiv \lim_{\rho\to\infty}\frac{1}{n}\sum_{I\in\mathcal{I}}\sum_{I\neq I'\in\mathcal{I}} \mathsf{P}_{\mathsf{e}}(S,\mathcal{A}^c|I',I) \times \mathsf{Pr}[g(I),g(I')]. \tag{12}$$

The following propositions quantify the error floors in $\mathsf{P}_{\mathsf{e}}^{\mathsf{EFC}}(\mathcal{A})$ and $\mathsf{P}_{\mathsf{e}}^{\mathsf{EFC}}(S,\mathcal{A}^c)$ as $\rho\to\infty$.

Proposition 1: In an EDAS aided SM system operating in an EFC, we have

$$\lim_{\rho\to\infty}\mathsf{P}_{\mathsf{e}}^{\mathsf{EFC}}(\mathcal{A}) = \frac{1}{n}\sum_{I\in\mathcal{I}}\sum_{I\neq I'\in\mathcal{I}}\frac{\zeta(I',I)}{N_{SM}}\mathsf{Pr}[g(I),g(I')], \tag{13}$$

where $\zeta(I',I) = d_I(I',I) + d_U(I',I)(N_{SM}-1)/N_{SM}$.

Proof: From (11), we have

$$\lim_{\rho\to\infty}\mathsf{P}_{\mathsf{e}}^{\mathsf{EFC}}(\mathcal{A}) = \frac{1}{n}\sum_{I\in\mathcal{I}}\sum_{I\neq I'\in\mathcal{I}}\left\{\lim_{\rho\to\infty}\mathsf{P}_{\mathsf{e}}(\mathcal{A}|I',I)\right\} \times \mathsf{Pr}[g(I),g(I')]. \tag{14}$$

Given that the antenna subset requested by the receiver is I and that used by the transmitter is I', an antenna index error would occur under two conditions:

1) When the transmitter activates an antenna that belongs to the set $(I\cap I')_I$;
2) When the transmitter activates an antenna that belongs to the set $I'\backslash(I\cap I')$.

Under condition 1), the antenna index error would happen with probability one as $\rho\to\infty$. This is so, since any antenna activated from the set $(I\cap I')_I$ would invariably be detected to be the same antenna but mapped to a different index in I. Under condition 2), the antenna index error would happen with probability $(N_{SM}-1)/N_{SM}$. This is so, since any antenna activated from the set $I'\backslash(I\cap I')$ would be detected to be any of the N_{SM} antennas with equal probability. Furthermore, condition 1) is encountered with a probability of $d_I(I',I)/N_{SM}$ and condition 2) occurs with probability $d_U(I',I)/N_{SM}$. Thus, we have

$$\lim_{\rho\to\infty}\mathsf{P}_{\mathsf{e}}(\mathcal{A}|I',I) = 1\cdot\frac{d_I(I',I)}{N_{SM}} + \frac{N_{SM}-1}{N_{SM}}\cdot\frac{d_U(I',I)}{N_{SM}}, \tag{15}$$

$$= \frac{d_I(I',I) + d_U(I',I)(N_{SM}-1)/N_{SM}}{N_{SM}}, \tag{16}$$

$$= \zeta(I',I)/N_{SM}. \tag{17}$$

This concludes the proof. ■

Proposition 2: In an EDAS-aided SM system operating in an EFC, we have

$$\lim_{\rho\to\infty}\mathsf{P}_{\mathsf{e}}^{\mathsf{EFC}}(S,\mathcal{A}^c) = \sum_{I\in\mathcal{I}}\sum_{I\neq I'\in\mathcal{I}}\frac{d_U(I',I)(M-1)}{N_{SM}^2 M} \times \mathsf{Pr}[g(I),g(I')]. \tag{18}$$

Proof: From (12), we have

$$\lim_{\rho\to\infty}\mathsf{P}_{\mathsf{e}}^{\mathsf{EFC}}(S,\mathcal{A}^c) = \frac{1}{n}\sum_{I\in\mathcal{I}}\sum_{I\neq I'\in\mathcal{I}}\left\{\lim_{\rho\to\infty}\mathsf{P}_{\mathsf{e}}(S,\mathcal{A}^c|I',I)\right\} \times \mathsf{Pr}[g(I),g(I')]. \tag{19}$$

Given that the antenna subset requested by the receiver is I and that used by the transmitter is I', a symbol error under the

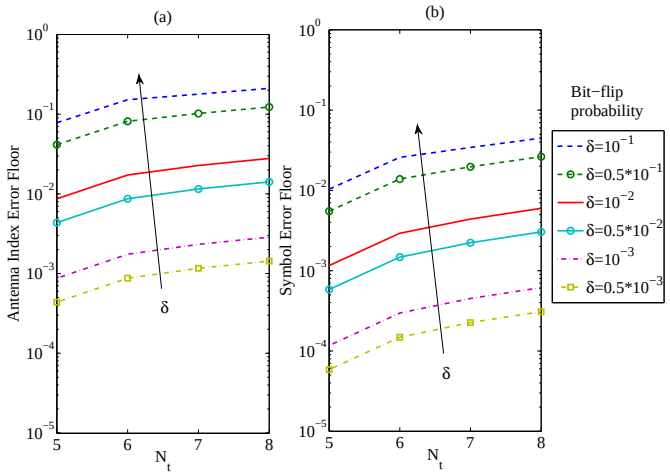

Fig. 2. Plot (a) depicts the variation in $\lim_{\rho\to\infty} \mathsf{P}_{\mathsf{e}}^{\mathsf{EFC}}(\mathcal{A})$ for different values of N_t and δ, while Plot (b) depicts the variation in $\lim_{\rho\to\infty} \mathsf{P}_{\mathsf{e}}^{\mathsf{EFC}}(S,\mathcal{A}^c)$, where M is taken to be 16. In both the plots N_{SM} is fixed to be 4.

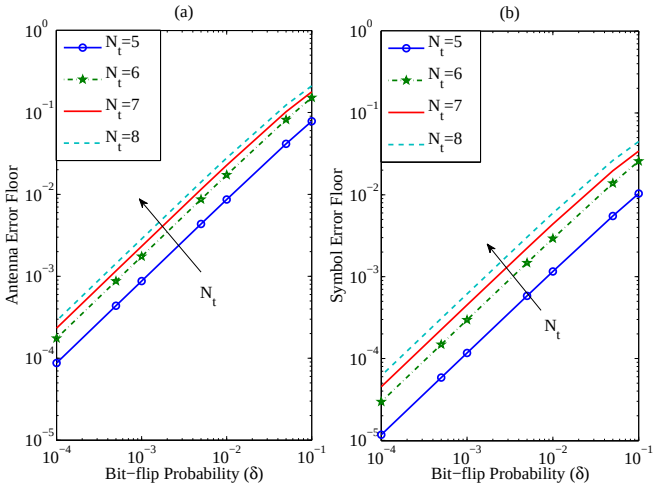

Fig. 3. Plot (a) depicts the variation in $\lim_{\rho\to\infty} \mathsf{P}_{\mathsf{e}}^{\mathsf{EFC}}(\mathcal{A})$ as a function of bit-flip error probability δ for various values of N_t, while Plot (b) depicts the variation in $\lim_{\rho\to\infty} \mathsf{P}_{\mathsf{e}}^{\mathsf{EFC}}(S,\mathcal{A}^c)$, where M is taken to be 16. In both the plots, N_{SM} is fixed to be 4.

condition that there is no antenna index error occurs, when the transmitter actives an antenna from the set $I'\backslash(I\cap I')$ and the receiver decodes it to be correct, whose probability is $1/N_{SM}$. Furthermore, the symbol error would occur with probability $(M-1)/M$, since all the symbols are equally likely to be in error. Furthermore, the probability of activating an antenna from the set $I'\backslash(I\cap I')$ is $d_U(I',I)/N_{SM}$. Thus, we have

$$\lim_{\rho\to\infty} \mathsf{P}_{\mathsf{e}}(S,\mathcal{A}^c|I',I) = \frac{1}{N_{SM}}\cdot\frac{d_U(I',I)}{N_{SM}}\cdot\frac{M-1}{M}. \quad (20)$$

This concludes the proof. ■

Figure 6 compares the error floor in $\mathsf{P}_{\mathsf{e}}^{\mathsf{EFC}}(\mathcal{A})$ and $\mathsf{P}_{\mathsf{e}}^{\mathsf{EFC}}(S,\mathcal{A}^c)$ as a function of N_t for various values of δ in a SM system having $N_{SM}=4$ and $M=16$. It is evident from Fig. 6 that $\lim_{\rho\to\infty} \mathsf{P}_{\mathsf{e}}^{\mathsf{EFC}}$ and $\lim_{\rho\to\infty} \mathsf{P}_{\mathsf{e}}^{\mathsf{EFC}}(S,\mathcal{A}^c)$ do not grow linearly with N_t, i.e. the increase in the number of antenna combinations $n=\binom{N_t}{N_{SM}}$ due to an increase in N_t does not result in a proportional growth in the error floor. This is due to the fact that as N_t increases, the number of illegitimate bit combinations amongst the m-bit sequences also increases. As a result, only a reduced number of m-bit sequences is utilized amongst the available 2^m bit combinations. Thus, effectively more bits are utilized for encoding each of the antenna combinations, as N_t increases. As a result the performance degradation is reduced. On the other hand, note that this would cause multiple retransmissions in the feedback link, hence resulting in an increased overhead. Furthermore, it is evident from Fig. 6 that $\lim_{\rho\to\infty} \mathsf{P}_{\mathsf{e}}^{\mathsf{EFC}}(S,\mathcal{A}^c)$ is significantly lower than $\lim_{\rho\to\infty} \mathsf{P}_{\mathsf{e}}^{\mathsf{EFC}}(\mathcal{A})$ and hence $\lim_{\rho\to\infty} \mathsf{P}_{\mathsf{e}}^{\mathsf{EFC}}(SM)$ is dominated by $\lim_{\rho\to\infty} \mathsf{P}_{\mathsf{e}}^{\mathsf{EFC}}(\mathcal{A})$.

Figure 3 compares the error floor in $\mathsf{P}_{\mathsf{e}}^{\mathsf{EFC}}(\mathcal{A})$ and $\mathsf{P}_{\mathsf{e}}^{\mathsf{EFC}}(S,\mathcal{A}^c)$ as a function of δ for various values of N_t in the aforementioned SM system. It is evident from Fig. 3 that the error floor in the forward link is directly proportional to the bit-flip probability δ in the feedback channel, regardless of the number of TAs N_t.

B. Optimized Signalling Assignment (OSA)

In this section, we present a simple optimization algorithm conceived for obtaining a bijective map $g:\mathcal{I}\to\mathcal{W}$ that reduces the error floor in the forward link due to EFC. Since the error floor in the forward link is dominated by $\lim_{\rho\to\infty} \mathsf{P}_{\mathsf{e}}^{\mathsf{EFC}}(\mathcal{A})$, we use it as our optimization metric in the proposed algorithm. The set of codewords $\mathcal{W}$ is assumed to contain the m-bit binary equivalent of the numbers from the set $\{0,1,2,\ldots,n-1\}$, which has one-to-one correspondence with the antenna subsets $\{I_1,I_2,I_3,\ldots,I_n\}$. We are interested in finding a bijective map $g:\mathcal{I}\to\mathcal{W}$ that solves

$$g^\star = \arg\min_g \lim_{\rho\to\infty} \mathsf{P}_{\mathsf{e}}^{\mathsf{EFC}}(\mathcal{A}), \quad (21)$$

$$= \arg\min_g \frac{1}{n}\sum_{I\in\mathcal{I}}\sum_{I\neq I'\in\mathcal{I}} \frac{\zeta(I',I)}{N_{SM}}\mathsf{Pr}[g(I),g(I')]. \quad (22)$$

Note that the number of possible bijective mappings can be extremely large even for modest values of N_t and N_{SM}. For example, when $N_t=6$ and $N_{SM}=4$, we have $n=15$ and the number of possible mappings will be $n!=15!=1.3077\times10^{12}$. Thus, we resort to a simple random sampling based algorithm for finding a reasonable solution to (22). The proposed OSA is presented in Algorithm 1. The optimized maps obtained from Algorithm 1 while considering an SM system having $N_{SM}=4$ and $N_t\in\{5,6\}$ are given in Table II. In case of $N_t=6$, the max_samples value in Algorithm 1 is taken to be 10^4. Figure 4 compares the attainable improvement in the error floor due to OSA in an SM system having $N_{SM}=4$ and $N_t\in\{5,6\}$. Note that although Algorithm 1 would improve the error floor in the forward link, it will not completely eliminate it. In the next section, we present selection verification algorithms that would help eliminate the error floor.

Algorithm 1 Signaling Assignment Optimization

Require: $k = 0$, max_samples, $\mathsf{EF}^\star = 1$, $\mathcal{I}$ and $\mathcal{W}$.
while $k <$ max_samples **do**
1. Compute a random bijective map $g : \mathcal{I} \rightarrow \mathcal{W}$.
2. Obtain $\mathsf{Pr}(g(I), g(I'))$.
3. Compute

$$\mathsf{EF} = \frac{1}{n} \sum_{I \in \mathcal{I}} \sum_{I \neq I' \in \mathcal{I}} \frac{\zeta(I', I)}{N_{SM}} \mathsf{Pr}(g(I), g(I')).$$

4.
if $\mathsf{EF} < \mathsf{EF}^\star$ **then**
$g^\star = g$,
$\mathsf{EF}^\star = \mathsf{EF}$.
end if
5. $k \leftarrow k + 1$.
end while
return $g^\star$

TABLE II
OPTIMIZED MAP g FOR $N_{SM} = 4$ CASE.

$\mathcal{I}$ ($N_t = 6$)	$\mathcal{W}$ ($N_t = 6$)	$\mathcal{I}$ ($N_t = 5$)	$\mathcal{W}$ ($N_t = 5$)
$I_1 = \{3, 4, 5, 6\}$	1100	$I_1 = \{1, 2, 3, 4\}$	010
$I_2 = \{2, 4, 5, 6\}$	0111	$I_2 = \{1, 2, 3, 5\}$	000
$I_3 = \{2, 3, 5, 6\}$	1010	$I_3 = \{1, 2, 4, 5\}$	001
$I_4 = \{2, 3, 4, 6\}$	1000	$I_4 = \{1, 3, 4, 5\}$	011
$I_5 = \{2, 3, 4, 5\}$	0001	$I_5 = \{2, 3, 4, 5\}$	100
$I_6 = \{1, 4, 5, 6\}$	1011		
$I_7 = \{1, 3, 5, 6\}$	1110		
$I_8 = \{1, 3, 4, 6\}$	1001		
$I_9 = \{1, 3, 4, 5\}$	0101		
$I_{10} = \{1, 2, 5, 6\}$	0100		
$I_{11} = \{1, 2, 4, 6\}$	0010		
$I_{12} = \{1, 2, 4, 5\}$	0110		
$I_{13} = \{1, 2, 3, 6\}$	0011		
$I_{14} = \{1, 2, 3, 5\}$	0000		
$I_{15} = \{1, 2, 3, 4\}$	1101		

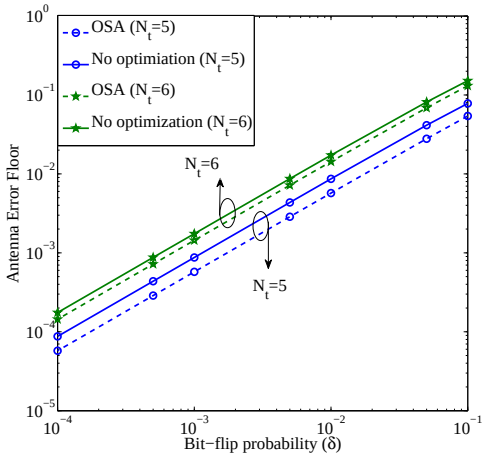

Fig. 4. Comparison of $\lim_{\rho \rightarrow \infty} \mathsf{P_e}^{\mathsf{EFC}}(\mathcal{A})$ as a function of bit-flip error probability δ in OSA and "No optimization" scenarios for $N_t \in \{5, 6\}$. The SM system is assumed to have $N_{SM} = 4$ in both the cases.

C. Proposed Selection Verification Algorithm for EDAS-aided SM Systems

In this section, we present an antenna subset selection verification algorithm for EDAS-aided SM systems in order to eliminate the error floor in the forward link. Specifically, we propose a pilot-aided selection verification (PSV), which is a generalization of the selection verification algorithm conceived for C-AS systems [6]. The proposed PSV scheme is described as follows:

1) Upon acquiring the channel state information, the receiver computes the set I_{ED} that obeys (2) and transmits this information to the transmitter.
2) Upon receiving the feedback information from the receiver, the transmitter chooses the set I' and sends p pilot symbols on each of the N_{SM} antennas present in the set I'. Let

$$\mathbf{Y}_k = \sqrt{\rho} \mathbf{h}_{i'_k} \mathbf{x}_p + \mathbf{N} \qquad \in \mathbb{C}^{N_r \times p},$$

for $1 \leq k \leq N_{SM}$ denote the received matrix corresponding to the pilot stream transmitted through the antenna $i'_k \in I'$, where $\mathbf{x}_p = [1, 1, \ldots, 1]$ is a p-length vector.
3) Since the receiver knows the pilot stream $\mathbf{x}_p$ *a priori*, it obtains an estimate $\hat{I}' = \{\hat{i}'_{i_1}, \hat{i}'_{i_2}, \ldots, \hat{i}'_{i_{N_{SM}}}\}$ of the actual antenna set used by the transmitter as

$$\hat{i}'_{i_k} = \arg \min_{i=1,2,\ldots,N_t} \|\mathbf{Y}_k - \sqrt{\rho} \mathbf{h}_i \mathbf{x}_p\|^2, \qquad (23)$$

for $1 \leq k \leq N_{SM}$.
4) The receiver performs data detection over the rest of the coherence period by considering $\hat{I}'$ as the antenna set used by the transmitter.

Proposition 3: The transmit diversity gain of the EDAS-aided SM system operating in an EFC at a bit-flip probability $\delta > 0$ and employing the PSV scheme is 1.

Proof: The proof is straightforward, which is provided here for the sake of completeness. Assuming $\hat{I}' = I'$[2], we have

$$\mathsf{P_e}^{\mathsf{EFC}}(SM) = \frac{1}{n} \sum_{I \in \mathcal{I}} \mathsf{P_e}(SM | \hat{I}' = I, I) \mathsf{Pr}[g(I), g(I)] + \frac{1}{n} \sum_{I \in \mathcal{I}} \sum_{I \neq \hat{I}' \in \mathcal{I}} \mathsf{P_e}(SM | \hat{I}', I) \mathsf{Pr}[g(I), g(\hat{I}')], \qquad (24)$$

which follows from (5). The first term in (24) has a transmit diversity order of $N_t - N_{SM} + 1$ [30], since this corresponds to the case where there is no feedback channel error. The second term corresponds to the case, where the antenna subset employed by the transmitter differs from that requested by the receiver. Since $\hat{I}'$ can be any of the antenna subsets in the set $\mathcal{I} \backslash I$, there exists an antenna set $\hat{I}' = I_k$ which corresponds to the diversity order one, i.e. $c_1/\rho < \mathsf{P_e}(SM | \hat{I}' = I_k, I) < c_2/\rho$. Thus, the dominant term in (24) scales as $1/\rho$. This concludes the proof. ■

[2]This is a valid assumption especially at high SNR values, since the PSV scheme ensures that the antenna subset used by the receiver is same as that employed by the transmitter.

IV. Simulation Results and Discussions

Simulation scenario: In all our simulations, we have employed at least 10^{t+1} bits for evaluating a bit error rate (BER) of 10^{-t}. The receiver is assumed to have perfect CSI in all the detection algorithms considered. In all the plots, the antenna index error refers to $\mathsf{P}_{\mathsf{e}}^{\mathsf{EFC}}(\mathcal{A})$ and the symbol error refers to $\mathsf{P}_{\mathsf{e}}^{\mathsf{EFC}}(S, \mathcal{A}^c)$. In all our simulation studies, the number of receive antennas is assumed to be $N_r = 2$. In all our PSV aided schemes, a training sequence length of $p = 1$ is assumed. The system parameters considered in our simulation studies presented in sections A-D given below are listed in Table III given in the next page.

A. Validation of Theoretical Results

In this section, we validate the theoretical results presented in *Proposition 1* and *Proposition 2*. Figure 5 compares $\mathsf{P}_{\mathsf{e}}^{\mathsf{EFC}}(\mathcal{A})$ and $\mathsf{P}_{\mathsf{e}}^{\mathsf{EFC}}(S, \mathcal{A}^c)$ to their asymptotic counterparts $\lim_{\rho\to\infty} \mathsf{P}_{\mathsf{e}}^{\mathsf{EFC}}(\mathcal{A})$ (13) and $\lim_{\rho\to\infty} \mathsf{P}_{\mathsf{e}}^{\mathsf{EFC}}(S, \mathcal{A}^c)$ (18) in an EDAS-aided SM system having $N_t = 5$, $N_{SM} \in \{2, 4\}$, and employing 16- and 32-QAM signal sets. The feedback channel is assumed to be erroneous with a bit-flip probability $\delta \in \{0.5 \times 10^{-1}, 0.5 \times 10^{-2}\}$. Specifically, Fig. 5(a) corresponds to $\mathsf{P}_{\mathsf{e}}^{\mathsf{EFC}}(\mathcal{A})$ and Fig. 5(b) corresponds to $\mathsf{P}_{\mathsf{e}}^{\mathsf{EFC}}(S, \mathcal{A}^c)$. It is evident from both Fig. 5(a) and Fig. 5(b) that the theoretical approximations of the asymptotics given in (13) and (18) coincide with the simulation results at high SNR values.

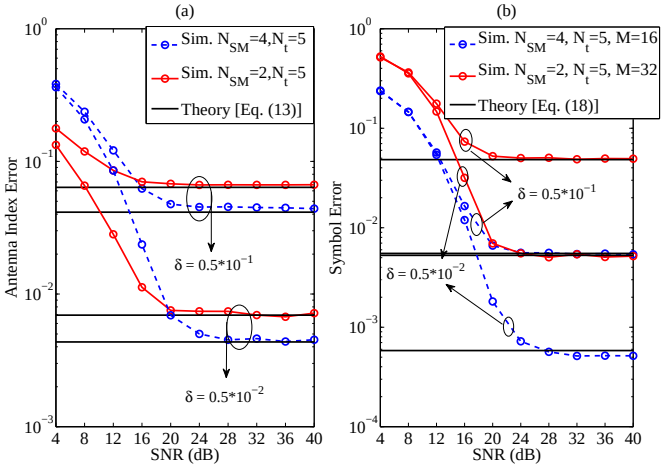

Fig. 5. Comparison of $\mathsf{P}_{\mathsf{e}}^{\mathsf{EFC}}(\mathcal{A})$ and $\mathsf{P}_{\mathsf{e}}^{\mathsf{EFC}}(S, \mathcal{A}^c)$ with their asymptotic counterparts in (13) and (18) for $\delta \in \{0.5 \times 10^{-1}, 0.5 \times 10^{-2}\}$ in an EDAS aided SM system having $N_t = 5$, $N_{SM} \in \{2, 4\}$, and employing 16- and 32-QAM signal sets.

Figure 6 compares $\mathsf{P}_{\mathsf{e}}^{\mathsf{EFC}}(\mathcal{A})$ and $\mathsf{P}_{\mathsf{e}}^{\mathsf{EFC}}(S, \mathcal{A}^c)$ to their asymptotic counterparts in (13) and (18) in an EDAS aided SM system having $N_{SM} = 4$, $N_t \in \{5, 7\}$, and employing 16-QAM signal set. The feedback channel is assumed to be erroneous with a bit-flip probability of $\delta = 0.5 \times 10^{-2}$. It is evident from Fig. 6 that the theoretical approximations of the asymptotics coincide with the simulation results at high SNR values. Note that the plots in Fig. 5 correspond to the case, where N_t is fixed and that in Fig. 6 correspond to the case where N_{SM} is fixed.

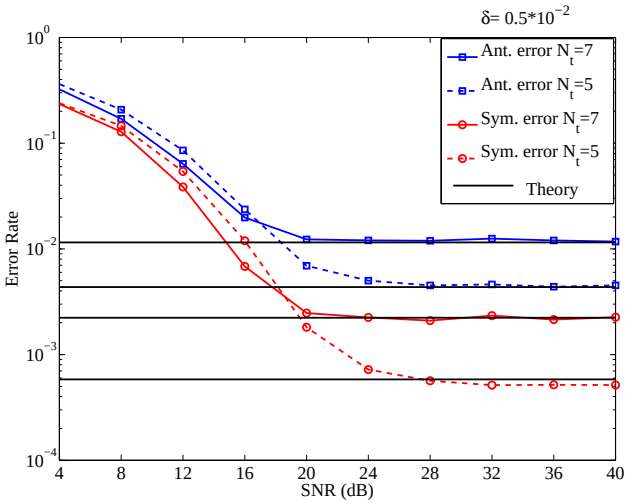

Fig. 6. Comparison of $\mathsf{P}_{\mathsf{e}}^{\mathsf{EFC}}(\mathcal{A})$ and $\mathsf{P}_{\mathsf{e}}^{\mathsf{EFC}}(S, \mathcal{A}^c)$ with their asymptotic counterparts in (13) and (18) for various values of N_t in an EDAS aided SM system having $N_{SM} = 4$, $N_t \in \{5, 7\}$, and operating in an EFC having $\delta = 0.5 \times 10^{-2}$ with 16-QAM signal set.

Figure 7 compares $\mathsf{P}_{\mathsf{e}}^{\mathsf{EFC}}(\mathcal{A})$ and $\mathsf{P}_{\mathsf{e}}^{\mathsf{EFC}}(S, \mathcal{A}^c)$ to their asymptotic counterparts in an EDAS-aided SM system having $N_{SM} = 4$, $N_t = 5$, and employing an M-QAM signal set, where $M \in \{16, 32, 64\}$. This corresponds to the case, where both N_t and N_{SM} are fixed. The feedback channel is assumed to be erroneous with a bit-flip probability of $\delta = 0.5 \times 10^{-2}$. It is seen from Fig. 7 that the theoretical approximations of the asymptotics given in (13) and (18) coincide with the simulation results at high SNR values. Similar observation holds for the lower modulation orders of $M = \{4, 8\}$ as well.

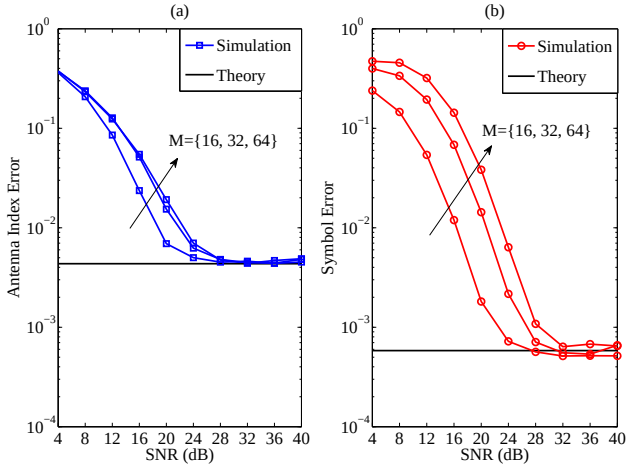

Fig. 7. Comparison of $\mathsf{P}_{\mathsf{e}}^{\mathsf{EFC}}(\mathcal{A})$ and $\mathsf{P}_{\mathsf{e}}^{\mathsf{EFC}}(S, \mathcal{A}^c)$ with their asymptotic counterparts in (13) and (18) for various M-QAM signal sets in an EDAS aided SM system having $N_{SM} = 4$, $N_t = 5$ and operating with an EFC having $\delta = 0.5 \times 10^{-2}$.

B. OSA vs. No Optimization

Figure 8 compares $\mathsf{P}_{\mathsf{e}}^{\mathsf{EFC}}(\mathcal{A})$ and $\mathsf{P}_{\mathsf{e}}^{\mathsf{EFC}}(S, \mathcal{A}^c)$ to the OSA and "No optimization" cases in an EDAS-aided SM system

TABLE III
SYSTEM PARAMETERS CONSIDERED IN OUR SIMULATION STUDIES.

	A	B	C	D
N_{SM}	$\{2, 4\}$	4	4	$\{1, 4\}$
N_t	$\{5, 7\}$	$\{5, 6\}$	7	5
N_r	2	2	2	2
M-QAM	$\{16, 32, 64\}$	16	16	$\{16, 32, 64\}$
δ	$\{10^{-1}, 10^{-2}\} \times 0.5$	10^{-2}	$\{0.1, 0.5 \times 10^{-2}\}$	0.5×10^{-1}

having $N_{SM} = 4$, $N_t \in \{5, 6\}$ and employing a 16-QAM signal set. The feedback channel is assumed to be erroneous with a bit-flip probability of $\delta = 10^{-2}$. Observe from Fig. 8(a) that there is an improvement in the error floor of $\mathsf{P}_{\mathsf{e}}^{\mathsf{EFC}}(\mathcal{A})$ in case of OSA compared to the "No optimization" case. Furthermore, it can be observed, from Fig. 8(b) that the $\mathsf{P}_{\mathsf{e}}^{\mathsf{EFC}}(S, \mathcal{A}^c)$ remains the same in both the cases. This is expected, since Algorithm 1 considers $\mathsf{P}_{\mathsf{e}}^{\mathsf{EFC}}(\mathcal{A})$ as its optimization metric.

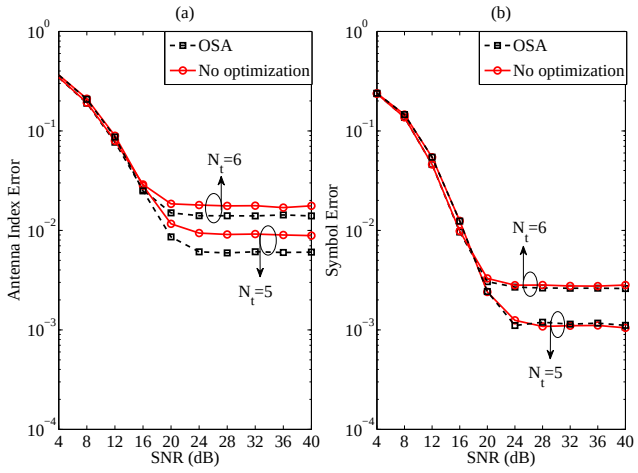

Fig. 8. Comparison of $\mathsf{P}_{\mathsf{e}}^{\mathsf{EFC}}(\mathcal{A})$ and $\mathsf{P}_{\mathsf{e}}^{\mathsf{EFC}}(S, \mathcal{A}^c)$ in an EDAS aided SM system employing OSA with its "No optimization" counterpart. The SM system is assumed to have $N_{SM} = 4$, $N_t \in \{5, 6\}$ and employing 16-QAM signal set, while operating in an EFC with $\delta = 10^{-2}$.

Furthermore, it is evident from Fig. 8(a) that having a larger N_t results in a poorer performance, when N_{SM} is fixed. This is expected, since any mismatch in the antenna subset would cause more antenna index errors, when $N_t \gg N_{SM}$. Note that in an ideal feedback channel, a larger N_t would enable attaining a higher transmit diversity order of $(N_t - N_{SM} + 1)$ [30], which does not hold in case of EFC. Furthermore, it is evident that although the OSA improves the error floor, it does not completely eliminate it. In the next section, we show that this issue can be overcome by our PSV scheme.

C. Performance of PSV

Figure 9 compares the BER performance of the EDAS aided SM system employing PSV to that of its counterparts having no selection verification. The SM system is assumed to have $N_{SM} = 4$, $N_t = 7$ and employing a 16-QAM signal set, while operating in an EFC at $\delta = \{0.1, 0.5 \times 10^{-2}\}$. It is evident from Fig. 9 that the PSV overcomes the error floor in the forward link caused by the EFC. Furthermore, it is evident from Fig. 9 that having a lower δ is essential to ensure that there is minimal degradation in the BER performance compared to that of the ideal feedback channel. It is also clear from Fig. 9 that the transmit diversity gain attained due to EDAS deteriorates when $\delta > 0$, as predicted by *Proposition 3*.

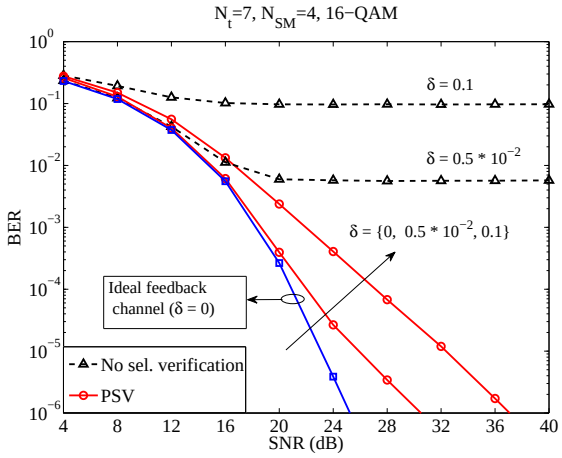

Fig. 9. Comparison of the BER performance of EDAS aided SM system employing PSV with its counterpart having no selection verification. The SM system is assumed to have $N_{SM} = 4$, $N_t = 7$ and employing 16-QAM signal set, while operating in an EFC with $\delta = \{0.1, 0.5 \times 10^{-2}\}$. The performance of the same system operating in an ideal feedback channel is also provided for comparison.

D. EDAS-SM vs. C-AS

Figure 10 compares the BER performance of our EDAS-aided SM system to that of C-AS, when no selection verification is employed. Both SM as well as the C-AS are assumed to have $N_t = 5$ and operate at a spectral efficiency of 6 and 7

bpcu. The EFC is assumed to have $\delta = 0.5 \times 10^{-1}$. It evident from both Fig. 10(a) and Fig. 10(b) that the EDAS aided SM system performs better than C-AS in both the cases. This is expected, since the impact of the antenna index mismatch on the forward link BER in case of C-AS is more severe compared to the case of EDAS aided SM.

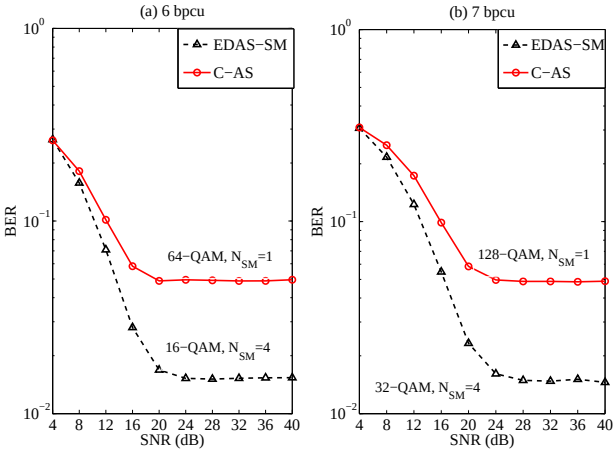

Fig. 10. Comparison of the BER performance of EDAS aided SM system with that of C-AS, when no selection verification is employed. Specifically, Plot (a) corresponds to the spectral efficiency of 6 bpcu and Plot (b) corresponds to that of 7 bpcu. Both the systems are assumed to have $N_t = 5$ and operating in an EFC having $\delta = 0.5 \times 10^{-1}$. The SM system is assumed to have $N_{SM} = 4$ and employing 16-QAM signal set, while the C-AS system is assumed have $N_{SM} = 1$ and employing 64-QAM signal set in order to attain a spectral efficiency of 6 bpcu. In case of 7 bpcu, the SM system and the C-AS system are assumed to employ 32-QAM and 128-QAM signal sets, respectively.

Figure 11 compares the BER performance of our EDAS aided SM system to that of C-AS, when both are employing the PSV scheme. The system parameters are the same as those of the no verification case considered above. It is seen from Fig. 11(a) and Fig. 11(b) that the EDAS-aided SM system outperforms the C-AS system. Specifically, at a BER of 10^{-5} the EDAS aided SM system is observed to provide an SNR gain of about 2.5dB compared to the C-AS system in case of 6 bpcu and about 3dB in case of 7 bpcu.

E. Challenges and Open Problems

As observed from Fig. 9 and *Proposition 3*, the EDAS-SM looses its advantage of high transmit diversity gain, when the feedback channel is erroneous, i.e $\delta > 0$. This is an important problem, which has to be solved in order to ensure that the key benefits of EDAS-SM are retained under the practical EFC conditions. In this paper, we have considered a fixed feedback signalling assignment, which does not depend on the instantaneous channel realization. It would be interesting to consider a channel-aware feedback signalling assignment as well as a codebook design and study the attainable improvements in the error floor as well as the transmit diversity gain of the EDAS-SM.

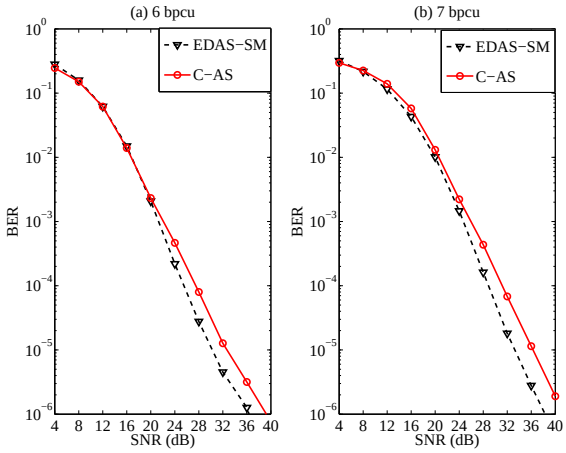

Fig. 11. Comparison of the BER performance of EDAS aided SM system with that of C-AS, when both are employing the PSV scheme. Specifically, Plot (a) corresponds to the spectral efficiency of 6 bpcu and Plot (b) corresponds to that of 7 bpcu. All the system parameters are same as that of Fig. 10.

V. Conclusions

In this paper, we have modeled the non-ideal feedback channel and studied its impact on the forward link in case of EDAS-SM, which has hitherto been studied only under ideal feedback channel conditions. The EFC was observed to cause error floors in the forward link owing to the antenna set mismatch between the transmitter and the receiver. The error floors associated with the spatial and conventional symbols were quantified theoretically and validated with the aid of simulation results. The error floor expressions derived were utilized for optimizing the feedback signalling assignment, which improved the error floor levels. Furthermore, the error floor issue in the forward link was overcome by the proposed PSV scheme. The transmit diversity order of EDAS-SM was observed to drop from $(N_t - N_r + 1)$ to one, when $\delta > 0$. Furthermore, our simulation results demonstrated that EDAS-SM outperforms the conventional antenna selection scheme with SNR gains as high as 3dB, even in the case of EFC.

VI. Acknowledgements

The authors acknowledge the use of the IRIDIS High Performance Computing Facility, and associated support services at the University of Southampton, in the completion of this work.

References

[1] S. Sanayei and A. Nosratinia, "Antenna selection in MIMO systems," *IEEE Commun. Mag.*, vol. 42, no. 10, pp. 68-73, Oct. 2004.

[2] D. Love, R. Heath, V. Lau, D. Gesbert, B. Rao, and M. Andrews, "An overview of limited feedback in wireless communication systems," *IEEE J. Sel. Areas Commun.*, Vol. 26, no. 8, pp. 1341-1365, Oct. 2008.

[3] R. Heath and A. Paulraj, "Antenna selection for spatial multiplexing systems based on minimum error rate," *in Proc. Int. Conf. Communications*, Helsinki, Finland, vol. 7, pp. 2276-2280, June 2001.

[4] A. Ghrayeb and T. M. Duman, "Performance analysis of MIMO systems with antenna selection over quasi-static fading channels," *IEEE Trans. Veh. Technol.*, vol. 52, no. 2, pp. 281-288, Mar. 2003.

[5] Z. Chen, J. Yuan, and B. Vucetic, "Analysis of transmit antenna selection/maximal-ratio combining in Rayleigh fading channels," *IEEE Trans. Veh. Technol.*, vol. 54, no. 4, pp. 1312-1321, Jul. 2005.

[6] Y. Li, N. B. Mehta, A. F. Molisch, and J. Zhang, "Optimal signalling and selection verification for single transmit-antenna selection," *IEEE Trans. Commun.*, vol. 55, no. 4, pp. 778-789, Apr. 2007.

[7] R. Mesleh, H. Haas, S. Sinanovic, C. Ahn and S. Yun "Spatial modulation," *IEEE Trans. Veh. Technol.*, vol. 57, no. 4, pp. 2228-2242, July 2008.

[8] M. Di Renzo, H. Haas and P. M. Grant, "Spatial modulation for multiple-antenna wireless systems - A Survey," *IEEE Commun. Magazine*, vol. 49, no. 12, pp. 182-191, Dec. 2011.

[9] M. Di Renzo, H. Haas, A. Ghrayeb, S. Sugiura and L. Hanzo, "Spatial modulation for generalized MIMO: challenges, opportunities, and implementation," *Proceedings of the IEEE*, vol. 102, no. 1, pp. 56-103, Jan. 2014.

[10] A. Stavridis, S. Sinanovic, M. Di Renzo and H. Haas, "Energy evaluation of spatial modulation at a multi-antenna base station," *2013 IEEE 78th Vehicular Technology Conference (VTC Fall)*, Las Vegas, NV, 2013.

[11] P. Som and A. Chockalingam, "Spatial modulation and space shift keying in single carrier communication," *IEEE 23rd International Symposium on Personal, Indoor and Mobile Radio Communications - (PIMRC)*, Sydney, NSW, pp. 1962-1967, 2012.

[12] R. Rajashekar, K.V.S. Hari and L. Hanzo, "Spatial modulation aided zero-padded single carrier transmission for dispersive channels," *IEEE Trans. Commun.*, vol. 61, no. 6, pp. 2318-2329, June 2013.

[13] L. He, J. Wang and J. Song, "Information-aided iterative equalization: A novel approach for single-carrier spatial modulation in dispersive channels," *IEEE Trans. Veh. Technol.*, vol. 66, no. 5, pp. 4448-4452, May 2017.

[14] R. Rajashekar, K.V.S. Hari, L. Hanzo, "Reduced-complexity ML detection and capacity-optimized training for spatial modulation systems," *IEEE Trans. Commun.*, vol. 62, no. 1, pp. 112-125, Jan. 2014.

[15] P. Yang, M. Di Renzo, Y. Xiao, S. Li and L. Hanzo, "Design guidelines for spatial modulation," *IEEE Communications Surveys & Tutorials*, vol. 17, no. 1, pp. 6-26, First quarter 2015.

[16] N. Ishikawa, R. Rajashekar, S. Sugiura and L. Hanzo, "Generalized-spatial-modulation-based reduced-RF-chain millimeter-wave communications," *IEEE Trans. Veh. Technol.*, vol. 66, no. 1, pp. 879-883, Jan. 2017.

[17] P. Yang, Y. Xiao, Y. L. Guan, Z. Liu, S. Li and W. Xiang, "Adaptive SM-MIMO for mmWave communications with reduced RF chains," to appear in *IEEE Journal on Selected Areas in Communications*. Available online - DOI:10.1109/JSAC.2017.2698899.

[18] P. Wolniansky, G. Foschini, G. Golden and R. Valenzuela, "V-BLAST: an architecture for realizing very high data rates over the rich-scattering wireless channel," *in Proc. International Symp. Signals, Syst., Electron.*, Pisa, Italy, pp. 295-300, Sep. 1998.

[19] V. Tarokh, N. Seshadri and A. R. Calderbank, "Space-time codes for high data rate wireless communication: performance criterion and code construction," *IEEE Trans. Inf. Theory*, vol. 44, no. 2, pp. 744-765, Mar 1998.

[20] S. M. Alamouti, "A simple transmit diversity technique for wireless communications," *IEEE Journal on Selected Areas in Communications*, vol. 16, no. 8, pp. 1451-1458, Oct 1998.

[21] E. Basar, U. Aygolu, E. Panayirci and H. V. Poor, "Space-time block coding for spatial modulation," *IEEE Trans. Commun.*, vol. 59, no. 3, pp. 823-832, Mar. 2011.

[22] R. Rajashekar and K.V.S. Hari, "Modulation diversity for spatial modulation using complex interleaved orthogonal design," *in Proc. IEEE TENCON 2012*, Nov. 2012, pp. 1-6.

[23] X. Li and L. Wang, "High rate space-time block coded spatial modulation with cyclic structure," *IEEE Commun. Lett.*, vol. 18, no. 4, pp. 532-535, Apr. 2014

[24] A. G. Helmy, M. Di Renzo and N. Al-Dhahir, "Enhanced-reliability cyclic generalized spatial-and-temporal modulation," *IEEE Commun. Lett.*, vol. 20, no. 12, pp. 2374-2377, Dec. 2016.

[25] P. Yang, Y. Xiao, L. Li, Q. Tang, Y. Yu and S. Li, "Link adaptation for spatial modulation with limited feedback," *IEEE Trans. Veh. Technol.*, vol. 61, no. 8, pp. 3808-3813, Oct. 2012.

[26] R. Rajashekar, K.V.S. Hari and L. Hanzo, "Antenna selection in spatial modulation systems," *IEEE Commun. Lett.*, vol. 17, no. 3, pp. 521-524, Mar. 2013.

[27] R. Rajashekar, K.V.S. Hari, K. Giridhar and L. Hanzo, "Performance analysis of antenna selection algorithms in spatial modulation systems with imperfect CSIR," *European Wireless 2013; 19th European Wireless Conference*, Guildford, UK, 2013, pp. 1-5.

[28] Z. Zhou, N. Ge and X. Lin, "Reduced-complexity antenna selection schemes in spatial modulation," *IEEE Commun. Lett.*, vol. 18, no. 1, pp. 14-17, Jan. 2014.

[29] N. Wang, W. Liu, H. Men, M. Jin, and H. Xu, "Further complexity reduction using rotational symmetry for EDAS in spatial modulation," *IEEE Commun. Lett.*, vol. 18, no. 10, pp. 1835-1838, Oct. 2014.

[30] R. Rajashekar, K.V.S. Hari and L. Hanzo, "Quantifying the transmit diversity order of Euclidean distance based antenna selection in spatial modulation," *IEEE Signal Proc. Lett.*, vol. 22, no. 9, pp. 1434-1437, Sept. 2015.

[31] Z. Sun, Y. Xiao, L. You, L. Yin, P. Yang and S. Li, "Cross-entropy-based antenna selection for spatial modulation," *IEEE Commun. Lett.*, vol. 20, no. 3, pp. 622-625, March 2016.

[32] P. Yang, Y. Xiao, Y. L. Guan, S. Li and L. Hanzo, "Transmit antenna selection for multiple-input multiple-output spatial modulation systems," *IEEE Trans. Commun.*, vol. 64, no. 5, pp. 2035-2048, May 2016.

[33] Z. Sun *et. al.*, "Transmit antenna selection schemes for spatial modulation systems: search complexity reduction and large-scale MIMO applications," to appear in *IEEE Trans. Veh. Technol.* Avaiable online - DOI:10.1109/TVT.2017.2696381.

[34] Y. Naresh and A. Chockalingam, "On media-based modulation using RF mirrors," *IEEE Trans. Veh. Technol.*, vol. 66, no. 6, pp. 4967-4983, June 2017.

[35] R. Rajashekar, K.V.S. Hari and L. Hanzo, "Transmit antenna subset selection for single and multiuser spatial modulation systems operating in frequency selective channels," submitted to *IEEE Trans. Veh. Technol.*. Available online: https://eprints.soton.ac.uk/411710/

[36] 3rd Generation Partnership Project, "Physical layer procedures(FDD)," Tech. Rep. 25.214, 2005.

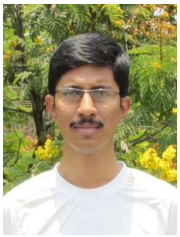

Rakshith Rajashekar (M'14) received the B.E. degree in electrical communication engineering from Visvesvaraya Technological University, Karnataka, India, in 2007. He received his Ph.D.from the Department of Electrical Communication Engineering, Indian Institute of Science (IISc), India, in 2014. He is presently working as a Research Fellow at the University of Southampton (UoS), UK. Before joining the UoS, he worked as a Senior Scientist at Broadcom Communications, Bangalore, India, from 2014 to 2015 and as a Systems Engineer at Accord Software & Systems, Bangalore, India, from 2007 to 2009. His research interests include diversity schemes in MIMO systems, differential communication, millimeter wave communication with a focus on space-time signal processing and coding.

K.V.S. Hari (M'92-SM'97-F'15) received the B.E. degree from Osmania University, Hyderabad, India, in 1983; the M.Tech. degree from the Indian Institute of Technology Delhi, New Delhi, India, in 1985; and the Ph.D. degree from the University of California at San Diego, La Jolla, CA, USA, in 1990. Since 1992, he has been with the Department of Electrical Communication Engineering, Indian Institute of Science, Bangalore, India, where he is currently a Professor and coordinates the activities of the Statistical Signal Processing Laboratory. He was an Affiliated Professor (2010-16) with the Department of Signal Processing, KTH Royal Institute of Technology, Stockholm, Sweden. He has been a Visiting Faculty Member with Stanford University, Stanford, CA, USA; KTH Royal Institute of Technology, Stockholm, Sweden; and Aalto University, Espoo, Finland (formerly Helsinki University of Technology). While at Stanford University, he worked on multiple-input multiple-output (MIMO) wireless channel modelling and co-authored the Worldwide Interoperability for Microwave Access standard on wireless channel models for fixed-broadband wireless communication systems, which proposed the Stanford University Interim channel models. He was also with the Defence Electronics Research Laboratory, Hyderabad, and the Research and Training Unit for Navigational Electronics, Osmania University. His research interests include the development of signal processing algorithms for MIMO wireless communication systems, sparse signal recovery problems, indoor positioning, assistive technologies for the elderly, and neuroscience. Dr. Hari was an Editor of Elsevier's EURASIP journal Signal Processing (2006-16) and the Senior Associate Editor of Springer's Indian Academy of Sciences journal SADHANA. He is an Academic Entrepreneur and a Cofounder of the company ESQUBE Communication Solutions, Bangalore. He received the Institution of Electronics and Telecommunication Engineers S. V. C. Aiya Award for Excellence in Telecom Education and the Distinguished Alumnus Award from the Osmania University College of Engineering, Hyderabad. He is a Fellow of the Indian NAE.

Lajos Hanzo (M'91-SM'92-F'04) (http://www-mobile.ecs.soton.ac.uk) FREng, FIEEE, FIET, Fellow of EURASIP, DSc received his degree in electronics in 1976 and his doctorate in 1983. In 2009 he was awarded the honorary doctorate "Doctor Honoris Causa" by the Technical University of Budapest. During his 38-year career in telecommunications he has held various research and academic posts in Hungary, Germany and the UK. Since 1986 he has been with the School of Electronics and Computer Science, University of Southampton, UK, where he holds the chair in telecommunications. He has successfully supervised about 100 PhD students, co-authored 20 John Wiley/IEEE Press books on mobile radio communications totalling in excess of 10,000 pages, published 1,500+ research entries at IEEE Xplore, acted both as TPC and General Chair of IEEE conferences, presented keynote lectures and has been awarded a number of distinctions. Currently he is directing a 100-strong academic research team, working on a range of research projects in the field of wireless multimedia communications sponsored by industry, the Engineering and Physical Sciences Research Council (EPSRC) UK, the European Research Council's Advanced Fellow Grant and the Royal Society's Wolfson Research Merit Award. He is an enthusiastic supporter of industrial and academic liaison and he offers a range of industrial courses.

Lajos is a Fellow of the Royal Academy of Engineering, of the Institution of Engineering and Technology, and of the European Association for Signal Processing. He is also a Governor of the IEEE VTS. During 2008-2012 he was the Editor-in-Chief of the IEEE Press and a Chaired Professor also at Tsinghua University, Beijing. He has 22,000+ citations. For further information on research in progress and associated publications please refer to http://www-mobile.ecs.soton.ac.uk.